symmetry

MDPI

Article

Strange Things in Bottom-to-Strange Decays: The Standard Model Turned Upside Down?

Martin Andersson [1], Alexander Mclean Marshall [2], Konstantinos A. Petridis [2,*] and Eluned Smith [3,*]

[1] Physics Institute, University of Zurich, 8057 Zurich, Switzerland; martin.andersson@cern.ch
[2] H.H. Wills Physics Laboratory, School of Physics, University of Bristol, Bristol BS8 1TL, UK; alex.marshall@cern.ch
[3] Department of Physics, Massachusetts Institute of Technology, Cambridge, MA 02139, USA
* Correspondence: konstantinos.petridis@cern.ch (K.A.P.); eluned@mit.edu (E.S.)

Abstract: The flavour anomalies are a set of experimental deviations from the Standard Model (SM) predictions in several observables involving decays of bottom quarks. In particular, tensions between theory and experiment in measurements involving a bottom quark decaying into a strange quark and a pair of muons have motivated much theoretical work to explore possible new physics explanations. This review summarises the tumultuous evolution of these tensions, focusing on the most recent experimental results and their implications for physics beyond the SM. We also discuss the prospects for future measurements and tests of the flavour anomalies at the LHC and other facilities.

Keywords: flavour physics; branching fraction; angular analysis; lepton flavour universality

Citation: Andersson, M.; Marshall, A.M.; Petridis, K.A.; Smith, E. Strange Things in Bottom-to-Strange Decays: The Standard Model Turned Upside Down? *Symmetry* **2024**, *16*, 638. https://doi.org/10.3390/sym16060638

Academic Editor: Francesco Renga

Received: 25 April 2024
Revised: 8 May 2024
Accepted: 10 May 2024
Published: 21 May 2024

1. Introduction

Hadrons are bound states of quarks, such as protons and neutrons, which can be described as bound states of up (u) and down (d) quarks. The proton is a uud bound state, and the neutron is a udd bound state. A neutron can decay into a proton through the decay $d \to uW$, where W is a virtual W boson, one of the mediators of the weak interaction.

Bottom, or B, hadrons that contain a bottom (b) quark existed very early on in the Universe and can be produced at particle colliders. Similar to the decay of a neutron into a proton, a B hadron will primarily decay into a D hadron containing a charm (c) quark through the process $b \to cW$. In contrast, the b quark cannot decay directly into an s quark through the process $b \to sZ$ or $b \to s\gamma$, where Z and γ denote electrically neutral mediators of the weak and electromagnetic interactions. Such transitions constitute an electrically neutral change in quark flavour, namely of a b quark into an s quark, known as a Flavour-Changing Neutral Current. Such FCNCs are forbidden at the tree level in the SM of particle physics owing to an accidental symmetry of the SM but can occur at the one-loop level. As such, $b \to s$ transitions are expected to occur at a far lower rate compared to $b \to c$ transitions.

The study of FCNC quark transitions has shaped the concepts and underlying symmetries that underpin the SM. Key examples include the inference of the existence of the c quark through the study of $K^0 \to \mu^+\mu^-$ decays [1]; the realisation of the large top-quark mass by measuring $B^0 \leftrightarrow \bar{B}^0$ oscillations [2]; and the exclusion of a multitude of theoretically favoured extension to the SM using $B_s^0 \to \mu^+\mu^-$ transitions [3–5].

The past decade has seen a rise in interest in FCNC processes involving the quark-level decay $b \to s\ell^+\ell^-$, where ℓ denotes an electron or muon lepton. For instance the decays $B^+ \to K^+\ell^+\ell^-$, $B^0 \to K^{*0}\ell^+\ell^-$, $B_s \to \phi\ell^+\ell^-$ all involve the same $b \to s\ell^+\ell^-$ transition and are collectively called electroweak penguin decays. An example of an SM contribution to the $B^0 \to K^{*0}\ell^+\ell^-$ decay is shown in Figure 1. Electroweak penguin decays are excellent probes for new fundamental particles or interactions. For instance, a new gauge boson or a leptoquark could mediate the $B^0 \to K^{*0}\ell^+\ell^-$ without the FCNC suppression that

exists for SM-mediated transitions [6–10], also shown in Figure 1. As such, the effects of any new physics could manifest in relatively large deviations in the properties of such decays compared to predictions of the SM, and such deviations could be observable with precision measurements.

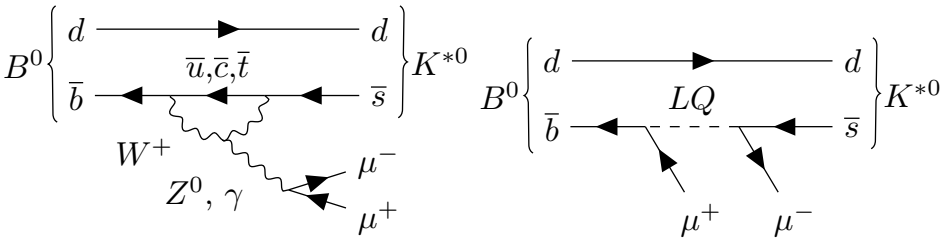

Figure 1. Example SM Feynman diagram of the decay $B^0 \to K^{*0}\mu^+\mu^-$ (**left**), and a potential new physics contribution including a leptoquark (**right**).

Only approximately one in a million B hadrons will undergo an electroweak penguin decay, therefore precision measurements of such processes can only be performed using extremely large samples of B hadrons. The B-factory experiments of BaBar and Belle pioneered the analyses of electroweak penguin decays in the B sector, but it was the LHC experiments of LHCb, and to a lesser extent, CMS and ATLAS, that offered a step change in precision by exploiting the immense samples of B hadrons produced at the LHC.

Since 2013, a coherent set of discrepancies from SM predictions have emerged in measurements involving $b \to s\ell^+\ell^-$ transitions. In particular, measurements of both branching fractions and angular distributions of $b \to s\mu^+\mu^-$ decays show consistent deviations from SM predictions across a range of final states. Measurements of the ratios of branching fractions between $b \to s\mu^+\mu^-$ and $b \to se^+e^-$ final states have also generated a lot of interest, as these observables are very precisely predicted and therefore have the potential to display clear signs of physics beyond the SM. This review cover measurements of all these $b \to s\ell^+\ell^-$ observables, including their various experimental challenges.

2. Theoretical Formalism

Under the assumption that particles beyond the SM have a mass larger than that of the known fundamental particles, one can employ an Effective Field Theory approach to compute the observables of $b \to s\ell^+\ell^-$ processes. Such an approach allows one to predict the effects of the SM or of new particles without adhering to a particular model, i.e., in a model-independent way. Using this approach, the effective Hamiltonian of a $b \to s\ell^+\ell^-$ process can be written as

$$\mathcal{H}_{\text{eff}} = \frac{-4G_F}{\sqrt{2}} V_{ts}^* V_{tb} \sum_{i=7,9,10,S,P} (\mathcal{C}_i \mathcal{O}_i + \mathcal{C}_i' \mathcal{O}_i'), \tag{1}$$

where the operators $\mathcal{O}_i$ encode the low-energy behaviour of the $b \to s\ell^+\ell^-$ process, and the Wilson coefficients $\mathcal{C}_i$ denote the complex-valued coupling strength of the particular operator. The factor G_F is the Fermi constant, and V_{ts} and V_{tb} are Cabbibo–Kobayashi–Maskawa (CKM) matrix elements. The various operators contributing to $\mathcal{H}_{\text{eff}}$ modify the angular momentum, parity, and charge-parity properties of the decay. The electromagnetic dipole operator is $\mathcal{O}_7$, the dilepton vector and axial-vector operators are denoted by $\mathcal{O}_9$ and $\mathcal{O}_{10}$, respectively, and the (pseudo)scalar operators are denoted by $\mathcal{O}_{P,S}$. The Quantum Chromodynamics (QCD) operators $\mathcal{O}_{1-6,8}$ mix through renormalisation with operators $\mathcal{O}_{7,9}$ giving rise to observables that are sensitive to effective operators $\mathcal{O}_{7,9}^{\text{eff}}$. The primed operators denote the contributions involving right-handed chirality quarks. As weak interactions only involve left-handed chirality particles and anti-particles, $\mathcal{C}_9' = \mathcal{C}_{10}' = 0$ in the SM and $\mathcal{C}_7'$ is suppressed by the ratio of quark masses m_s/m_b compared to $\mathcal{C}_7$. Any contribution from new physics at higher energy scales than the SM, will manifest itself in values of Wilson coefficients that are different from their SM predictions. As such,

measurements of the properties of $b \to s\ell^+\ell^-$ decays are sensitive to any new physics model that introduces operators appearing in $\mathcal{H}_{\text{eff}}$. The size of the Wilson coefficient depends on both the coupling strength of the new particle to the particles of the SM, as well as the mass of the new physics particle.

Therefore, measurements of $b \to s\ell^+\ell^-$ transitions cannot pinpoint the mass of new physics particles. However, the energy-scale reach only depends on the precision of the measurement and of the SM prediction of the $b \to s\ell^+\ell^-$ process. Therefore, as a consequence of Heisenberg's uncertainty principle, measurements of $b \to s\ell^+\ell^-$ decays are sensitive to new particles with masses far larger than what can be reached by searching for new particles directly produced at the LHC.

Quarks cannot be observed in isolation but rather as constituents of hadronic bound states. This means that the study of $b \to s\ell^+\ell^-$ processes involves the transition of a bottom hadron (e.g., $B^{0,\pm}$, B_s^0, Λ_b^0) into a hadron containing a strange quark (e.g., $K^{0,\pm}$, $K^{*(\pm,0)}$, ϕ, Λ). As such, observables associated with $b \to s\ell^+\ell^-$ decays are not just influenced by the presence of high-energy particles but also by low-energy strong interactions that determine the behaviour of hadronic bound states. The collection of these low-energy QCD effects is encapsulated in the operators $\mathcal{O}^{(\prime)}_{7,9,10}$ and are described through form factors that depend on the squared invariant-mass of the dilepton system, q^2. These form factors cannot be computed using perturbative techniques. Instead, methods such as Lattice QCD, which is most precise at high q^2, and Light-Cone Sum Rules, which are most precise at low q^2, are employed to compute the form factors involved in $b \to s\ell^+\ell^-$ transitions. The uncertainties associated with the computation of these form factors directly impact the sensitivity of measurements extracting the Wilson coefficients and thus of new physics effects. The impact of such uncertainties can be reduced by measuring observables in different regions of q^2; assessing the presence of new physics through measurements of the entire set of observables that describe a particular decay, including their correlations; or constructing observables that are less sensitive or completely insensitive to form-factor uncertainties such as the P_i' [11] and R_K [12] observables discussed in later sections.

Decays involving a $b \to s\ell^+\ell^-$ transition receive contributions from $b \to c\bar{c}s$ amplitudes, where the $c\bar{c}$ is an intermediate state that decays to a pair of leptons via the electromagnetic interaction $c\bar{c} \to \ell^+\ell^-$. As the initial and final states between these two processes are the same, their quantum mechanical amplitudes will interfere. Theory predictions account for these $b \to c\bar{c}s \to \ell^+\ell^-s$ amplitudes as form-factors that introduce q^2-dependent shifts to the Wilson coefficients $\mathcal{C}_9$ and/or $\mathcal{C}_7$. An example of a $b \to c\bar{c}s \to \ell^+\ell^-s$ transition is the decay $B^+ \to K^+J/\psi$ where the J/ψ is a $c\bar{c}$ bound state that can decay to a dilepton pair. The $B^+ \to K^+J/\psi \to K^+\ell^+\ell^-$ branching fraction is 100 times larger than that of the $B^+ \to K^+\ell^+\ell^-$ decay. Although the $B^+ \to K^+J/\psi \to K^+\ell^+\ell^-$ process is mostly localised around the narrow dilepton mass distribution of the J/ψ hadron, i.e., around 3 GeV, the $b \to c\bar{c}(\to \ell^+\ell^-)s$ amplitude is so much larger than that of the $b \to s\ell^+\ell^-$ transition that its effect can be significant even for offshell J/ψ hadrons [13]. Given the multitude of $c\bar{c}$ hadrons that can decay to a dilepton pair, the correct determination of the $b \to c\bar{c}s \to \ell^+\ell^-s$ amplitudes and their associated uncertainty is paramount in order to use $b \to s\ell^+\ell^-$ measurements as probes for effects beyond the SM. Over the past five years, there has been significant development of the theory's techniques to compute these non-local hadronic contributions that rely on Lattice QCD, LCSR computations, and data.

3. Experimental Aspects

Current studies of B hadrons rely on production from proton collisions at the LHC or electron–positron collisions at the SuperKEKB collider. The former is the source of B hadrons for the LHCb [14], CMS [15], and ATLAS [16] experiments, and the latter is the source of B mesons for the Belle II experiment [17]. A key characteristic of ground-state B hadrons, such as $B^{0,\pm}$, B_s^0, and Λ_b^0 is their relatively long lifetime of $\mathcal{O}(10^{-12}\ s)$. This is because ground-state B hadrons can only decay via the weak interaction which predominantly involves the quark-mixing matrix elements (CKM matrix) V_{cb} and V_{ub},

which are small in magnitude. Collider experiments exploit this long lifetime, coupled with the effect of the Lorentz boost in the detector frame, to identify B hadron decays through the displacement of their decay-vertex from other vertices in the collision: B hadrons are produced at the LHC with an average momentum of 100 GeV/c resulting in the displacement of the B decay vertex being of the order of centimetres.

All experiments that study $b \to s\ell^+\ell^-$ processes employ machine learning approaches to suppress combinatorial backgrounds, that is, backgrounds formed by the combination of particles from the same or different B hadron decays in the same event. At the LHC, the B hadrons originating from the same event have well-separated decay products owing to the large flight distances in the lab frame. This results in better discrimination of combinatorial backgrounds, compared to B factory experiments where the lower Lorentz boost of the B hadrons results in a large spatial overlap of decay products.

The study of a particular $b \to s\ell^+\ell^-$ process requires the ability to distinguish between that signal process and other decays that could form a dangerous background with similar kinematic distributions to the signal but with different types of particles in the final state. For instance, in the LHC experiments, the study of the process $B^0 \to K^+\pi^-\mu^+\mu^-$ could be contaminated by a multitude of other $b \to s\ell^+\ell^-$ or fully hadronic transitions, such as the decays $B_s \to K^+K^-\mu^+\mu^-$, $\Lambda_b \to pK^+\mu^+\mu^-$, and $B^0 \to K^+\pi^-\pi^+\pi^-$. Therefore, distinguishing between muons, pions, protons, and kaons is crucial to reducing such cross-feed (or peaking) backgrounds. This is achieved in the LHCb and Belle II experiments using dedicated particle-identification detectors sensitive to the speed of particles. In the LHCb experiment, particle identification information results in kaons being correctly identified with 95% efficiency for a 5% pion-to-kaon misidentification probability, muons with 97% efficiency for a 1–3% pion-to-muon misidentification probability, and electrons with 90% efficiency for a 5% electron-to-hadron misidentification probability.

The production cross-section of B hadrons at the LHC is a factor of 10^5 larger than that of B factory experiments, such as Belle II. However, the more challenging hadronic environment of the LHC means B hadron candidates are selected with significantly lower efficiency than at B factories. What is more, at the LHC the full set of B hadrons can be studied, whereas B factories primarily produce B^0 and B^+ mesons.

The presence of muons in $b \to s\mu^+\mu^-$ decays allows for the efficient selection of signal events with low muon momentum threshold requirements while suppressing the LHC's large hadronic background rate. This means that experiments like LHCb have a higher sensitivity to $b \to s\mu^+\mu^-$ processes than B factory experiments. For $b \to se^+e^-$ processes, the electrons deposit energy in the detector's electromagnetic calorimeters. This means that LHC experiments must employ high thresholds on the electron's transverse energy to suppress hadronic backgrounds that also deposit significant energy in the electromagnetic calorimeter of LHCb. In addition, the loss of energy from Bremsstrahlung radiation results in more electrons being swept out of the detector acceptance. The combination of these effects results in the reconstruction efficiency of LHCb for $b \to se^+e^-$ being a factor of five lower than for $b \to s\mu^+\mu^-$. In contrast, B factory experiments select and reconstruct $b \to s\mu^+\mu^-$ and $b \to se^+e^-$ candidates with similar efficiencies.

4. Branching Fraction Measurements

The simplest observable property of $b \to s\ell^+\ell^-$ transitions that is sensitive to new physics contributions is the probability of the transition, i.e., the branching fraction. At the LHC, branching fractions of $b \to s\ell^+\ell^-$ processes are measured relative to a normalisation decay channel with a well-known branching fraction that has been measured at B factory experiments. This approach has the benefit of cancelling the dependence on both the B hadron production cross-section and the total number of proton–proton collisions (integrated luminosity), which come with sizeable uncertainties. Additionally, normalisation channels are chosen to minimise experimental systematic uncertainties related to the knowledge of the reconstruction efficiency of the signal process. As such, normalisation channels are chosen to have a similar topology to the decay of interest. For instance, the measurement

of the $B^+ \to K^+\mu^+\mu^-$ branching fraction is measured relative to $B^+ \to K^+J/\psi$, where subsequently, the J/ψ intermediate state decays to $\mu^+\mu^-$.

The most precise branching fraction measurements of $b \to s\mu^+\mu^-$ decays have been performed by the LHCb collaboration and form the main focus of the discussion. These branching fraction measurements are performed in bins of q^2, which provides additional information on the characteristics of any new physics effects. Binning schemes are constructed to exclude regions of q^2 dominated by the $b \to c\bar{c}(\to \ell^+\ell^-)s$ contributions discussed in Section 2.

Binned differential branching fraction measurements of $b \to s\mu^+\mu^-$ decays at LHCb include the following: $B^0 \to K^{*0}\mu^+\mu^-$ [18], $B^\pm \to K^\pm\mu^+\mu^-$ [19], $B^0 \to K^0\mu^+\mu^-$ [19], $B^\pm \to K^{*\pm}\mu^+\mu^-$ [19], $B_s^0 \to \phi\mu^+\mu^-$ [20], and $\Lambda_b^0 \to \Lambda\mu^+\mu^-$ [21]. The results of these measurements are presented along with SM predictions in Figure 2. There are complementary measurements from CMS and the B factories for some of these same channels; however, the precision achieved is not competitive [22–24]. These branching fraction measurements consistently fall below the predictions across q^2. The overall significance of the measurements from SM predictions is up to 4σ, dampened by the large uncertainties in these predictions originating from local form factors, which are correlated both between bins and across channels. Systematic uncertainties originating from limited knowledge of normalisation mode branching fractions can be significant in these measurements, larger even than the statistical uncertainty. Therefore, improvements to the measurements of these normalisation channels from the B factories will significantly enhance the precision LHCb can achieve with future data sets.

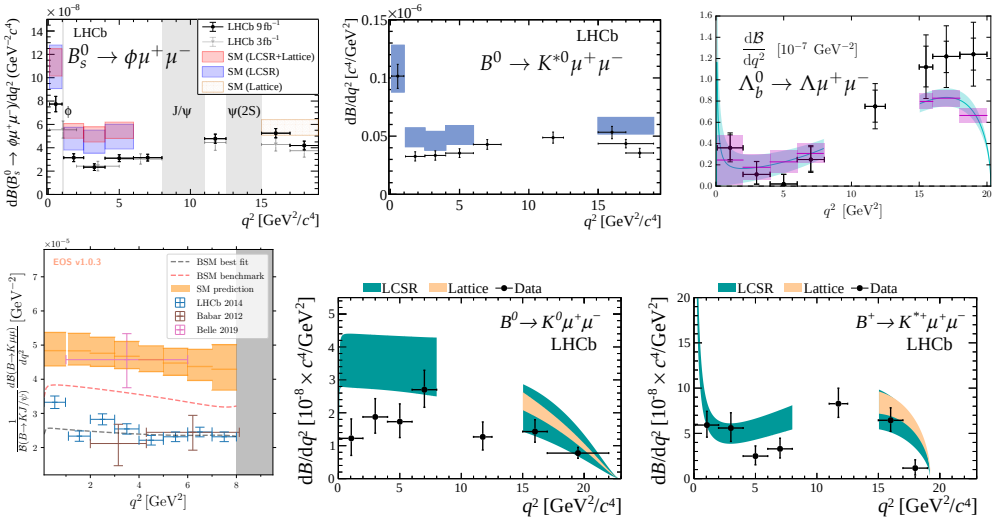

Figure 2. Overview of branching fraction measurements, taken from Refs. [18–21,25,26]. The SM predictions are given by the solid boxes or bands and are taken from Refs. [6,25–31].

Predictions of inclusive $B \to X_s\mu^+\mu^-$ branching fractions, where X_s can be any hadron containing an s quark, have smaller hadronic uncertainties than their exclusive counterparts [32]. However, performing inclusive measurements is experimentally challenging and measurements to date have relied on extrapolation from exclusive measurements [33,34]. At high q^2, kinematic constraints mean that only two decays dominate the inclusive decay rate, making the "semi-inclusive" rate obtained from summing up exclusive modes more robust. Similarly to the exclusive measurements in the high-q^2 region, the semi-inclusive decay rate is observed to lie below SM predictions at the level of 2σ, see Figure 3.

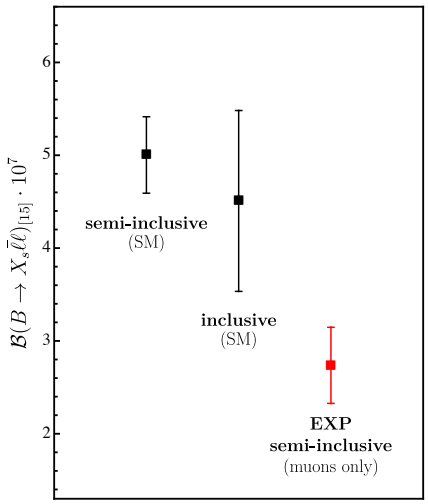

Figure 3. A comparison of inclusive and semi-inclusive combinations of measurements with an SM prediction in the q^2 region above 15 GeV^2 [35].

The LHCb collaboration has published an analysis of the full q^2 spectrum of $B^\pm \to K^\pm \mu^+ \mu^-$ parameterising the decay rate in terms of the Wilson coefficients $\mathcal{C}_9$ and $\mathcal{C}_{10}$ and hadronic form factors [36]. The model also includes all known spin-1 vector resonance contributions across the entire q^2 spectrum. The results of this analysis display a similar tension with the SM as the binned results of Ref. [19].

Studying neutral lepton channels is only possible at the B factories. The first evidence (3.5σ deviation from a background-only hypothesis) for $B^\pm \to K^\pm \nu\bar{\nu}$ was recently presented by the Belle II collaboration [37] indicating a 2.7σ tension with the SM, and the branching fraction was measured to be $(2.7 \pm 0.7) \times 10^{-5}$ relative to the SM prediction of $(5.58 \pm 0.37) \times 10^{-6}$ [38]. This measurement is inclusive of all lepton flavours with the only final state particle being reconstructed being the $K^\pm$.

The $B_s^0 \to \mu^+ \mu^-$ branching fraction is a benchmark measurement in the search for new physics. The lack of a hadron in the final state results in an additional suppression of the SM amplitude compared to the aforementioned $b \to s\ell^+\ell^-$ processes and an even more precise branching fraction prediction. Measurements of the $B_s^0 \to \mu^+ \mu^-$ branching fraction by the LHCb, CMS, and ATLAS collaborations are compatible with the SM prediction [3–5], providing stringent constraints on new physics models. A dedicated review article on this and other similar processes can be found in Ref. [39]. Similarly, a dedicated review of searches for charged Lepton-Flavour Violation is presented in Ref. [40]. An observation of LFV in decays of B hadrons would be irrefutable evidence of beyond-the-SM physics.

5. Angular Analyses

5.1. q^2 Binned Angular Analyses

Angular analyses measure the differential decay rate as a function of q^2 as well as the decay angles between the final state particles $\vec{\Omega}$, describing the full available phase space for a decay. For the decay of a B meson into a spin-1 hadron and two leptons, such as $B \to K^* \mu^+ \mu^-$, the differential decay rate depends on twelve q^2-dependent observables, $S_i(q^2)$, that are built out of bilinear combinations of the decay amplitudes. These observables encode the different Lorentz structures of the decay and depend on both new physics (Wilson coefficients) and hadronic contributions (form factors). Angular analyses of $B \to K^* \ell^+ \ell^-$ transitions therefore offer more information on the underlying structure of any new physics. An added benefit is that angular observables suffer from smaller theoretical uncertainties than branching fractions. As shown in Equation (2), each $S_i(q^2)$ function is multiplied by a unique spherical harmonic function, $f_i(\vec{\Omega})$, of the angles between the decay products. These functions arise from the different angular momentum configurations of the final state.

$$\frac{1}{\Gamma}\frac{d\Gamma(B \to K^*\ell^+\ell^-)}{dq^2 d\vec{\Omega}} \propto \sum_i S_i(q^2) f_i(\vec{\Omega}). \quad (2)$$

Angular observables are extracted in bins of q^2 by fitting the angular distributions in each bin independently. An accurate and unbiased extraction of these observables requires precise knowledge of detector effects. The dependence of the detector efficiency as a function of all the phase-space variables that characterise the decay is obtained using simulated signal decays and is taken into account. Angular analyses have been performed in the following decays: $B^0 \to K^{*0}\mu^+\mu^-$ [41–44], $B^0 \to K^{*0}e^+e^-$ [44,45], $B^+ \to K^{*+}\mu^+\mu^-$ [46,47], $B_s \to \phi\mu^+\mu^-$ [48], $B^+ \to K^+\mu^+\mu^-$ [49,50], and $\Lambda_b \to \Lambda\mu^+\mu^-$ [21]. The most precise extraction of the angular observables in Equation (2) is from the LHCb analysis of the $B^0 \to K^{*0}\mu^+\mu^-$ mode.

Figure 4 shows a subset of the measured angular observables of $B^0 \to K^{*0}\mu^+\mu^-$ decays alongside their SM predictions. The observables shown are S_5, A_{FB}, and P_5', where A_{FB} corresponds to $\frac{3}{4}S_{6s}$ and represents the forward–backward asymmetry of the dimuon system. The observable P_5' is a parameterised version of S_5. The P_5' observable has been constructed such that it exhibits a reduced dependency on hadronic contributions. The values of angular observables of $B^0 \to K^{*0}\mu^+\mu^-$ measured at LHCb exhibit a $\sim 3\sigma$ tension with SM predictions, and a similar tension exists in the angular analysis of $B^+ \to K^{*+}\mu^+\mu^-$.

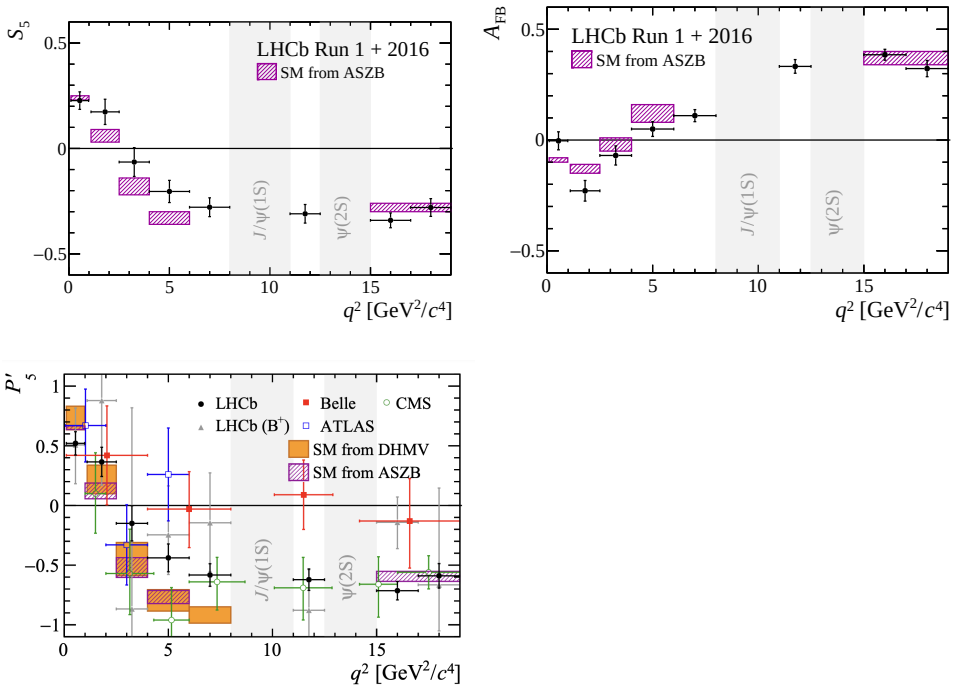

Figure 4. Measurements of the observables S_5, $S_{6s} \equiv \frac{4}{3}A_{FB}$, and P_5' in $B \to K^{*0}\mu^+\mu^-$ decays. The upper row shows results from Ref. [41] only. The lower row shows results from Refs. [41–44,46]. The solid boxes denote the SM predictions from Refs. [6,27] (**upper row**) and Refs [13,51] (**lower row**).

5.2. q^2 Unbinned Angular Analyses

The tensions between measurements and SM predictions in both angular and branching fraction measurements of $b \to s\mu^+\mu^-$ decays observed by the LHCb collaboration could either be due to beyond-the-SM physics or unaccounted hadronic contributions. In particular, computations of $b \to c\bar{c}s \to \mu^+\mu^-s$ have been recently brought into question as they can mimic new physics contributions in the observables P_5' and A_{FB}, as well as the branching fraction measurements discussed in Section 4. To that end, recent theoretical developments have enabled data-driven measurements of both new physics and hadronic effects directly from the data [52,53]. By analysing the angular and q^2 distribution continuously (rather than in bins) in q^2, using a model of the hadronic contributions in a limited region of q^2, the LHCb collaboration performed a direct measurement of the new

physics contributions to the Wilson coefficients and of the $b \to c\bar{c}s \to \mu^+\mu^- s$ hadronic amplitudes [54]. A similar preliminary analysis was also performed using a different model of the $b \to c\bar{c}s \to \mu^+\mu^- s$ hadronic amplitudes across the entire q^2 range [55]. As shown in Figure 5, both methods give compatible results for both the hadronic contributions and the Wilson coefficients which exhibit a deviation in the dimuon Wilson coefficient $\mathcal{C}_9$ at the level of 2σ.

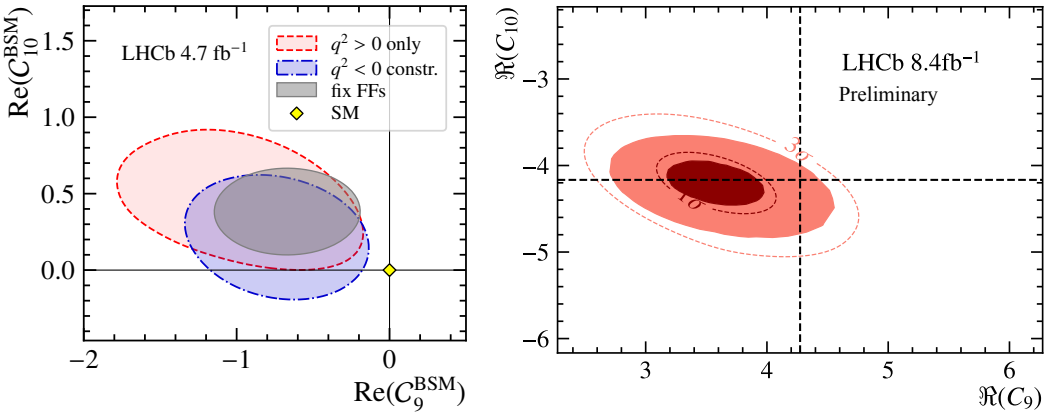

Figure 5. Results of q^2 unbinned angular analyses of $B^0 \to K^{*0}\mu^+\mu^-$ decays in terms of the dimuon vector ($\mathcal{C}_9$) and axial-vector ($\mathcal{C}_{10}$) Wilson coefficients using two different data-driven models of $b \to c\bar{c}s \to \mu^+\mu^- s$ contributions [54,55].

6. Tests of Lepton Flavour Universality

In the SM, couplings of gauge bosons to lepton are independent of lepton flavour. This is an accidental symmetry in the SM and will not necessarily hold in the presence of new physics. The lepton universal nature of the SM implies that $b \to s\ell\ell$ transitions should have the same decay rate into all three different lepton species, up to phase-space effects due to the differences in lepton masses. The Lepton Flavour Universality (LFU) ratios, R_{H_s}, are observables constructed to test LFU in data. Within the context of $b \to s\ell^+\ell^-$ transitions, so far, the most precise tests of LFU have involved first- and second-generation leptons, i.e., between electrons and muons. Therefore, the prominent LFU ratios in $b \to s\ell\ell$ transitions are defined as

$$R_{H_s} = \frac{\int_{q^2_{min}}^{q^2_{max}} \frac{d\mathcal{B}(H_b \to H_s \mu^+\mu^-)}{dq^2} dq^2}{\int_{q^2_{min}}^{q^2_{max}} \frac{d\mathcal{B}(H_b \to H_s e^+e^-)}{dq^2} dq^2}, \tag{3}$$

where H_s is a hadron containing an s quark and H_b a b quark. The LFU ratios are measured in bins of q^2 excluding the regions dominated by the charmonium resonant decays $J/\psi \to \ell^+\ell^-$ and $\psi(2S) \to \ell^+\ell^-$, which are known to obey LFU. From a theoretical point of view, these LFU ratios allow for the cancellation of the large lepton flavour universal hadronic uncertainties associated with branching fraction measurements. From an experimental point of view, the LFU ratios can be measured as a ratio of ratios, where each lepton-flavour specific branching fraction is measured relative to a normalisation mode that is known to be lepton flavour-universal, such as $B^+ \to J/\psi K^+$. Such an approach allows for the cancellation of experimental systematic uncertainties related to the understanding of electron- and muon-specific reconstruction and detector efficiencies. This is the technique employed by the LHCb collaboration. For example, the LFU ratio R_K is measured as follows:

$$R_K = \frac{N_{K\mu\mu}}{N_{Kee}} \cdot \frac{N_{KJ/\psi(\to ee)}}{N_{KJ/\psi(\to \mu\mu)}} \cdot \frac{\epsilon_{Kee}}{\epsilon_{K\mu\mu}} \cdot \frac{\epsilon_{KJ/\psi(\to \mu\mu)}}{\epsilon_{KJ/\psi(\to ee)}}, \tag{4}$$

where the N terms are the various numbers of reconstructed signal events, and the ϵ terms are the various detection efficiencies.

The LHCb experiment has performed the most precise tests of LFU in $b \to s\ell^+\ell^-$ transitions, with the most sensitive individual measurement being that of R_K. Until 2022, R_K and R_{K^*} were measured to be below the SM, a trend that was observed consistently across LFU measurements at LHCb. In 2021, the LHCb collaboration reported evidence of LFU violation in $B^+ \to K^+\ell^+\ell^-$ decays, which was, however, short-lived. A reanalysis of R_K and an update with four times more data of R_{K^*} by the LHCb collaboration resulted in measurements compatible with SM predictions [56]. The change in the central values of the measurement was primarily due to a reduction in, and a better understanding of, backgrounds involving the misidentification of hadrons as leptons. Whereas background from $B^+ \to K^+\pi^-\pi^-$ decays was previously considered, contributions from inclusive $B \to h^+h^-eX$ decays, where X can be any particle, along with other more complex misidentification patterns of hadronic decays, were not.

The most precise measurements of LFU observables in $b \to s\ell^+\ell^-$ transitions are summarised in Figure 6.

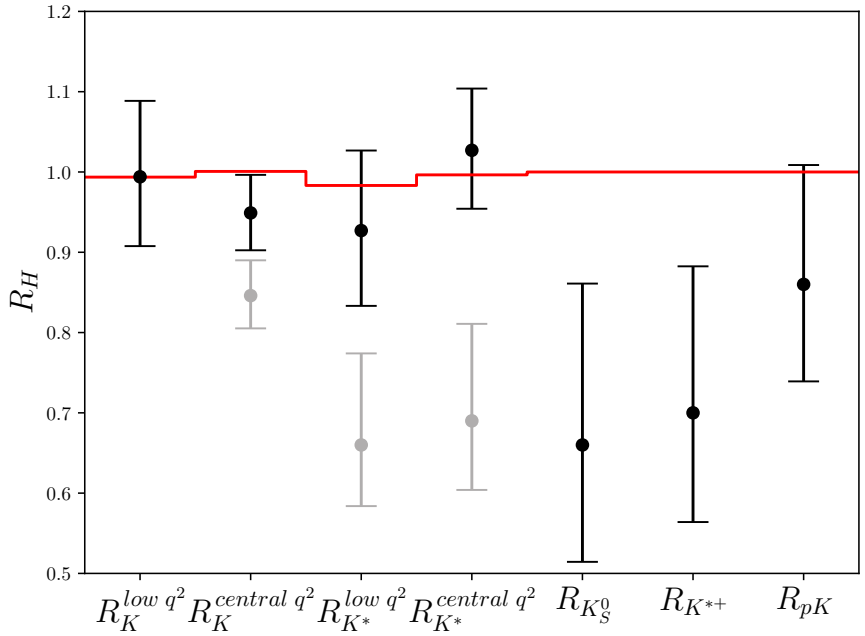

Figure 6. Presented in black are the most up-to-date LFU results from LHCb [56–58], with the SM prediction for each observable in red. Legacy LHCb results of Refs. [59,60] are presented in grey for easy comparison. Results from Belle, BaBar, and CMS are excluded for clarity; these can be found within Refs. [24,61–63].

7. Discussion

Different $b \to s\ell^+\ell^-$ observables offer complementary sensitivity to the underlying Wilson coefficients characterising any new physics effects as shown in Table 1. Thus, whilst tensions exist with the SM in measurements on individual observables, a global significance is necessary to assess the coherence of these measurements and to assess a combined level of compatibility with the SM. Multiple theory groups perform these global fit studies, using different formulations of the hadronic contributions in $b \to s\ell^+\ell^-$ decays [10,26,64,65], and all fits are in good agreement. An example of such a global fit from Ref. [10] is shown in Figure 7. In this example, the fit was performed to the vector- and axial-vector dimuon Wilson coefficients $\mathcal{C}_9$ and $\mathcal{C}_{10}$ using the experimental measurements discussed in this review as inputs. The result pointed to a significant new-physics contribution to the $\mathcal{C}_9$ dimuon Wilson coefficient with a 4σ significance in this two-parameter fit [10]. When considering all relevant Wilson coefficients in the fit [66], the global significance to the SM was found to be 3.4σ [10]. There are well-motivated and highly predictive extensions to the SM that can explain the observed tensions in the data.

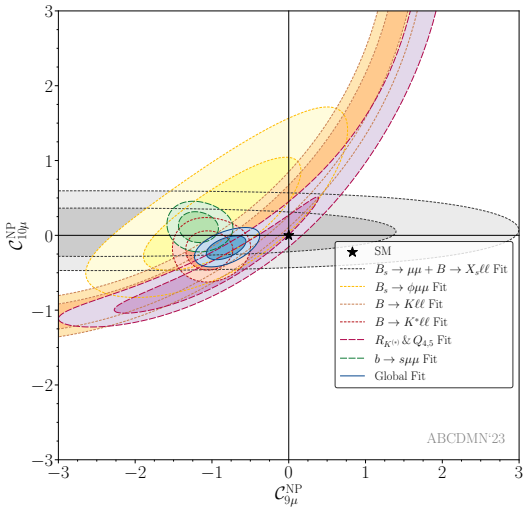

Figure 7. Example global fit for the muon-specific Wilson coefficients $\mathcal{C}_{9\mu}$ and $\mathcal{C}_{10\mu}$ (here presented as $\mathcal{C}^{NP}_{i\mu} = \mathcal{C}_{i\mu} - \mathcal{C}^{SM}_{i\mu}$), multiple limits are presented including various combinations of different observables, from Ref. [10].

Table 1. Sensitivity to different Wilson coefficients from observables measured in different types of $b \to s\ell^+\ell^-$ decays. The column labelled $B \to V\ell^+\ell^-$ denotes decays with a spin-1 vector hadron in the final state; the column $B \to P\ell^+\ell^-$ denotes decays with a spin-0 pseudoscalar hadron in the final state; and the column $B \to \ell^+\ell^-$ denotes fully leptonic $b \to s\ell^+\ell^-$ transitions. The number of ticks is proportional to the sensitivity of a given decay to a particular Wilson coefficient.

	$B \to V\ell^+\ell^-$	$B \to P\ell^+\ell^-$	$B \to \ell^+\ell^-$
$\mathcal{C}_7^{(\prime)}$	✔✔	✔	X
$\mathcal{C}_9^{(\prime)}$	✔✔	✔✔	X
$\mathcal{C}_{10}^{(\prime)}$	✔✔	✔✔	✔✔
$\mathcal{C}_S^{(\prime)}$	✔	✔	✔✔
$\mathcal{C}_P^{(\prime)}$	✔	✔	✔✔

Alternative explanations for the anomalies in $b \to s\ell^+\ell^-$ transitions are related to potentially underestimated hadronic contributions in the SM predictions of these decays. In particular, contributions from charm-hadron rescattering of the form $B \to D_s D^* \to K\mu^+\mu^-$, where the D_s is a bound state of a charm and anti-strange quark and the D^* is an excited state of a charm hadron, have been suggested as the potential culprit of the tension in $\mathcal{C}_9$ [67]. Although this claim remains unsubstantiated, there is now a concerted theoretical and experimental effort to try to understand the level at which underestimated hadronic effects could account for the anomaly.

8. Future Directions and Conclusions

Additional data from LHCb and Belle II experiments have started to arrive at an ever-increasing rate, culminating with the high-luminosity phase of the LHC planned to begin at the end of this decade. The role of these larger datasets in resolving the $b \to s\ell^+\ell^-$ anomalies can be divided into two parts. The first part involves a set of measurements that could provide the incontrovertible evidence required to claim the existence of a new fundamental particle or interaction behind the anomalies.

- The new physics models put forward for explaining the $b \to s\ell^+\ell^-$ anomalies predict a two-order of magnitude enhancement of the $b \to s\tau^+\tau^-$ decay rate relative to the SM [68]. This prediction originates from connecting the $b \to s\ell^+\ell^-$ anomalies with LFU tests in $B \to D^{(*)}\tau\nu_\tau$ and $B \to D^{(*)}\mu\nu_\mu$ decays that exhibit a 3σ tension with SM predictions [69–77]. Searches for $b \to s\tau^+\tau^-$ processes are challenging at LHCb

due to the presence of neutrinos stemming from the subsequent τ decays even for much-enhanced signal decay rates. The Belle II experiment is ideally suited for such measurements owing to the knowledge of the e^+e^- collision energy and the hermetic detector design that allows for the detection of the presence of neutrinos through missing energy in the collision.

- Larger datasets will also enable precise measurements of new physics effects that give rise to CP violation in $b \to s\ell^+\ell^-$ transitions. By analysing $B^0 \to K^{*0}\mu^+\mu^-$ and $\bar{B}^0 \to \bar{K}^{*0}\mu^+\mu^-$ decays separately, searches for complex-valued Wilson coefficients, and therefore sources of CP violation beyond the SM, can be pursued. The presence of a significant CP violation in $b \to s\ell^+\ell^-$ transitions would be a clear indication of new physics.

The second part involves measurements that provide additional information in order to enable the separation of hadronic from new-physics effects in $b \to s\mu^+\mu^-$ decays.

- Angular analyses of $B^0 \to K^{*0}\mu^+\mu^-$ and similar decays in ever-narrowing bins of q^2 can provide significant insight into the potential effect of hadronic contributions. New-physics effects in $\mathcal{C}_9$ should be consistent across different q^2 bins, in contrast to potential unaccounted hadronic effects. Similarly , new-physics effects in $\mathcal{C}_9$ should be consistent across different K^{*0} helicity amplitudes, in contrast to $b \to c\bar{c}s \to \mu^+\mu^-s$ amplitudes [78]. Measurements in small q^2 bins with high precision from the current and future runs of the LHC therefore have the potential to decouple new physics from unaccounted hadronic effects.
- Decays mediated via $b \to d\ell^+\ell^-$ transitions have an extra suppression (CKM suppression) in the SM with respect to their $b \to s\ell^+\ell^-$ counterpart. This additional suppression makes $b \to d\ell^+\ell^-$ transitions even more sensitive probes of new physics and stand to benefit the most from the large datasets collected over the following decades. If the deviations in $b \to s\ell^+\ell^-$ transitions are due to new physics with different quark couplings compared to the SM (i.e., not minimally flavour-violating), then large effects may be present in $b \to d\ell^+\ell^-$ transition. So far, only two $b \to d\ell^+\ell^-$ modes have been observed [79,80]. Additional data will allow for a broad physics program of $b \to d\ell^+\ell^-$ measurements, including angular analyses, LFU tests, and CP violation measurements. Testing the different amounts of CP violation between $b \to d\ell^+\ell^-$ and $b \to s\ell^+\ell^-$ decays can provide useful input on potential unaccounted $b \to c\bar{c}s \to \mu^+\mu^-s$ contributions owing to an approximate SM symmetry between $b \to c\bar{c}s$ and $b \to c\bar{c}d$ amplitudes.

In conclusion, the study of $b \to s\ell^+\ell^-$ decays remains a fruitful playground for exploring phenomena beyond the SM. Over the past decade, the increased experimental precision in a wide set of measurements, coupled with breakthroughs in hadronic computations from the theory community, has resulted in a coherent tension with SM predictions. The expected data from upcoming runs of the LHC, coupled with the unique capabilities of the Belle II experiment, will provide the information required to discern whether the $b \to s\ell^+\ell^-$ anomalies are due to unaccounted-for hadronic effects or the presence of new physics.

Author Contributions: All authors contributed equally to the writing and editing of this article. All authors have read and agreed to the published version of the manuscript.

Funding: This research received no external funding.

Data Availability Statement: No new data were created or analysed in this study. Data sharing is not applicable to this article.

Conflicts of Interest: All authors are members of the LHCb collaboration.

Abbreviations

The following abbreviations are used in this manuscript:

SM	Standard Model
FCNC	Flavour-Changing Neutral Current
LHC	Large Hadron Collider
CKM	Cabbibo–Kobayashi–Maskawa
QCD	Quantum Chromodynamics
LFU	Lepton Flavour Universality

References

1. Glashow, S.L.; Iliopoulos, J.; Maiani, L. Weak Interactions with Lepton-Hadron Symmetry. *Phys. Rev. D* **1970**, *2*, 1285–1292. [CrossRef]
2. Albrecht, H.; Andam, A.; Binder, U.; Böckmann, P.; Gläser, R.; Harder, G.; Nippe, A.; Schäfer, M.; Schmidt-Parzefall, W.; Schröder, H.; et al. Observation of B^0-B^0 Mixing. *Phys. Lett. B* **1987**, *192*, 245–252. [CrossRef]
3. Tumasyan, A.; Adam, W.; Andrejkovic, J.; Bergauer, T.; Chatterjee, S.; Damanakis, K.; Dragicevic, M.; Escalante Del Valle, A.; Hussain, P.; Jeitler, M.; et al. Measurement of the $B_S^0 \to \mu^+\mu^-$ decay properties and search for the $B^0 \to \mu^+\mu^-$ decay in proton-proton collisions at $\sqrt{s} = 13$ TeV. *Phys. Lett. B* **2023**, *842*, 137955. [CrossRef]
4. Aaij, R.; Abellán Beteta, C.; Ackernley, T.; Adeva, B.; Adinolfi, M.; Afsharnia, H.; Aidala, C.A.; Aiola, S.; Ajaltouni, Z.; Akar, S.; et al. Measurement of the $B_s^0 \to \mu^+\mu^-$ decay properties and search for the $B^0 \to \mu^+\mu^-$ and $B_s^0 \to \mu^+\mu^-\gamma$ decays. *Phys. Rev. D* **2022**, *105*, 012010. [CrossRef]
5. Aaboud, M.; Aad, G.; Abbott, B.; Abbott, D.C.; Abdinov, O.; Abeloos, B.; Abhayasinghe, D.K.; Abidi, S.H.; AbouZeid, O.S.; Abraham, N.L.; et al. Study of the rare decays of B_s^0 and B^0 mesons into muon pairs using data collected during 2015 and 2016 with the ATLAS detector. *J. High Energy Phys.* **2019**, *2019*, 98. [CrossRef]
6. Altmannshofer, W.; Straub, D.M. New physics in $b \to s$ transitions after LHC run 1. *Eur. Phys. J. C* **2015**, *75*, 382. [CrossRef]
7. Beaujean, F.; Bobeth, C.; van Dyk, D. Comprehensive Bayesian analysis of rare (semi)leptonic and radiative B decays. *Eur. Phys. J. C* **2014**, *74*, 2897; Erratum in *Eur. Phys. J. C* **2014**, *74*, 3179. [CrossRef] [PubMed]
8. Descotes-Genon, S.; Matias, J.; Virto, J. Understanding the $B \to K^*\mu^+\mu^-$ Anomaly. *Phys. Rev. D* **2013**, *88*, 074002. [CrossRef]
9. Algueró, M.; Capdevila, B.; Descotes-Genon, S.; Matias, J.; Novoa-Brunet, M. $b \to s\ell^+\ell^-$ global fits after R_{K_S} and $R_{K^{*+}}$. *Eur. Phys. J. C* **2022**, *82*, 326. [CrossRef]
10. Algueró, M.; Biswas, A.; Capdevila, B.; Descotes-Genon, S.; Matias, J.; Novoa-Brunet, M. To (b)e or not to (b)e: No electrons at LHCb. *Eur. Phys. J. C* **2023**, *83*, 648. [CrossRef]
11. Descotes-Genon, S.; Hurth, T.; Matias, J.; Virto, J. Optimizing the basis of $B \to K^*ll$ observables in the full kinematic range. *J. High Energy Phys.* **2013**, *2013*, 137. [CrossRef]
12. Hiller, G.; Kruger, F. More model-independent analysis of $b \to s$ processes. *Phys. Rev. D* **2004**, *69*, 074020. [CrossRef]
13. Khodjamirian, A.; Mannel, T.; Pivovarov, A.A.; Wang, Y.M. Charm-loop effect in $B \to K^{(*)}\ell^+\ell^-$ and $B \to K^*\gamma$. *J. High Energy Phys.* **2010**, *2010*, 89. [CrossRef]
14. Alves, A.A.; Andrade, L.M.; Barbosa-Ademarlaudo, F.; Bediaga, I.; Cernicchiaro, G.; Guerrer, G.; Lima, H.P.; Machado, A.A.; Magnin, J.; Marujo, F.; et al. The LHCb Detector at the LHC. *JINST* **2008**, *3*, S08005; Also published by CERN Geneva in 2010. [CrossRef]
15. Chatrchyan, S.; Hmayakyan, G.; Khachatryan, V.; Sirunyan, A.M.; Adolphi, R.; Anagnostou, G.; Brauer, R.; Braunschweig, W.; Esser, H.; Feld, L.; et al. The CMS experiment at the CERN LHC. The Compact Muon Solenoid experiment. *JINST* **2008**, *3*, S08004; Also published by CERN Geneva in 2010. [CrossRef]
16. Aad, G.; Bentvelsen, S.; Bobbink, G.J.; Bos, K.; Boterenbrood, H.; Brouwer, G.; Buis, E.J.; Buskop, J.J.F.; Colijn, A.P.; Dankers, R.; et al. The ATLAS Experiment at the CERN Large Hadron Collider. *JINST* **2008**, *3*, S08003; Also published by CERN Geneva in 2010. [CrossRef]
17. Kou, E.; Urquijo, P.; Altmannshofer, W.; Beaujean, F.; Bell, G.; Beneke, M.; Bigi, I.I.; Bishara, F.; Blanke, M.; Bobeth, C.; et al. The Belle II Physics Book. *Prog. Theor. Exp. Phys.* **2019**, *2019*, 123C01. [CrossRef]
18. Aaij, R.; Adeva, B.; Adinolfi, M.; Ajaltouni, Z.; Akar, S.; Albrecht, J.; Alessio, F.; Alexander, M.; Ali, S.; Alkhazov, G.; et al. Measurements of the S-wave fraction in $B^0 \to K^+\pi^-\mu^+\mu^-$ decays and the $B^0 \to K^*(892)^0\mu^+\mu^-$ differential branching fraction. *J. High Energy Phys.* **2016**, *2016*, 47; Erratum in *J. High Energy Phys.* **2017**, *2017*, 142. [CrossRef]
19. Aaij, R.; Adeva, B.; Adinolfi, M.; Affolder, A.; Ajaltouni, Z.; Albrecht, J.; Alessio, F.; Alexander, M.; Ali, S.; et al. Differential branching fractions and isospin asymmetries of $B \to K^{(*)}\mu^+\mu^-$ decays. *J. High Energy Phys.* **2014**, *2014*, 133. [CrossRef]
20. Aaij, R.; Beteta, C.A.; Ackernley, T.; Adeva, B.; Adinolfi, M.; Afsharnia, H.; Aidala, C.A.; Aiola, S.; Ajaltouni, Z.; Akar, S.; et al. Branching Fraction Measurements of the Rare $B_s^0 \to \phi\mu^+\mu^-$ and $B_s^0 \to f_2'(1525)\mu^+\mu^-$-Decays. *Phys. Rev. Lett.* **2021**, *127*, 151801. [CrossRef]
21. Aaij, R.; Adeva, B.; Adinolfi, M.; Affolder, A.; Ajaltouni, Z.; Akar, S.; Albrecht, J.; Alessio, F.; Alexander, M.; Ali, S.; et al. Differential branching fraction and angular analysis of $\Lambda_b^0 \to \Lambda\mu^+\mu^-$ decays. *J. High Energy Phys.* **2015**, *2015*, 115; Erratum in *J. High Energy Phys.* **2018**, *2018*, 145. [CrossRef]

22. Khachatryan, V.; Sirunyan, A.M.; Tumasyan, A.; Adam, W.; Asilar, E.; Bergauer, T.; Brandstetter, J.; Brondolin, E.; Dragicevic, M.; Erö, J.; et al. Angular analysis of the decay $B^0 \to K^{*0}\mu^+\mu^-$ from pp collisions at $\sqrt{s} = 8$ TeV. *Phys. Lett. B* **2016**, *753*, 424–448. [CrossRef]
23. Aubert, B.; Barate, R.; Bona, M.; Boutigny, D.; Couderc, F.; Karyotakis, Y.; Lees, J.; Poireau, V.; Tisserand, V.; Zghiche, A.; et al. Measurements of branching fractions, rate asymmetries, and angular distributions in the rare decays $B \to K\ell^+\ell^-$ and $B \to K^*\ell^+\ell^-$. *Phys. Rev. D* **2006**, *73*, 092001. [CrossRef]
24. Hayrapetyan, A.; Erbacher, R.; Carrillo Montoya, C.A.; Newbold, D.M.; Carvalho, W.; Karunarathna, N.; Górski, M.; Sommerhalder, M.; Lindsey, C.; Parmar, N.; et al. Test of lepton flavor universality in $B^{\pm} \to K^{\pm}\mu^+\mu^-$ and $B^{\pm} \to K^{\pm}e^+e^-$ decays in proton-proton collisions at $\sqrt{s} = 13$ TeV. *arXiv* **2024**, arXiv:2401.07090. [CrossRef]
25. Detmold, W.; Meinel, S. $\Lambda_b \to \Lambda\ell^+\ell^-$ form factors, differential branching fraction, and angular observables from lattice QCD with relativistic b quarks. *Phys. Rev. D* **2016**, *93*, 074501. [CrossRef]
26. Gubernari, N.; Reboud, M.; van Dyk, D.; Virto, J. Improved theory predictions and global analysis of exclusive $b \to s\mu^+\mu^-$ processes. *J. High Energy Phys.* **2022**, *2022*, 133. [CrossRef]
27. Bharucha, A.; Straub, D.M.; Zwicky, R. $B \to V\ell^+\ell^-$ in the Standard Model from light-cone sum rules. *J. High Energy Phys.* **2016**, *2016*, 98. [CrossRef]
28. Horgan, R.R.; Liu, Z.; Meinel, S.; Wingate, M. Lattice QCD calculation of form factors describing the rare decays $B \to K^*\ell^+\ell^-$ and $B_s \to \phi\ell^+\ell^-$. *Phys. Rev. D* **2014**, *89*, 094501. [CrossRef]
29. Parrott, W.G.; Bouchard, C.; Davies, C.T.H. B→K and D→K form factors from fully relativistic lattice QCD. *Phys. Rev. D* **2023**, *107*, 014510. [CrossRef]
30. Bobeth, C.; Hiller, G.; van Dyk, D. More Benefits of Semileptonic Rare B Decays at Low Recoil: CP Violation. *J. High Energy Phys.* **2011**, *2011*, 67. [CrossRef]
31. Bobeth, C.; Hiller, G.; van Dyk, D.; Wacker, C. The Decay $B \to K\ell^+\ell^-$ at Low Hadronic Recoil and Model-Independent $\Delta B = 1$ Constraints. *J. High Energy Phys.* **2012**, *2012*, 107. [CrossRef]
32. Huber, T.; Hurth, T.; Jenkins, J.; Lunghi, E.; Qin, Q.; Vos, K.K. Phenomenology of inclusive $\overline{B} \to X_s\ell^+\ell^-$ for the Belle II era. *J. High Energy Phys.* **2020**, *2020*, 88. [CrossRef]
33. Iwasaki, M.; Itoh, K.; Aihara, H.; Abe, K.; Abe, K.; Adachi, I.; Asano, Y.; Aushev, T.; Bahinipati, S.; Bakich, A.M.; et al. Improved measurement of the electroweak penguin process $B \to X_s l^+ l^-$. *Phys. Rev. D* **2005**, *72*, 092005. [CrossRef]
34. Lees, J.; Poireau, V.; Tisserand, V.; Grauges, E.; Palano, A.; Eigen, G.; Stugu, B.; Brown, D.N.; Kerth, L.; Kolomensky, Y.G.; et al. Measurement of the $B \to X_s l^+ l^-$ branching fraction and search for direct CP violation from a sum of exclusive final states. *Phys. Rev. Lett.* **2014**, *112*, 211802. [CrossRef]
35. Isidori, G.; Polonsky, Z.; Tinari, A. Semi-inclusive $b \to s\bar{\ell}\ell$ transitions at high q^2. *arXiv* **2023**, arXiv:2305.03076. [CrossRef]
36. Aaij, R.; Adeva, B.; Adinolfi, M.; Ajaltouni, Z.; Akar, S.; Albrecht, J.; Alessio, F.; Alexander, M.; Ali, S.; Alkhazov, G.; et al. Measurement of the phase difference between short- and long-distance amplitudes in the $B^+ \to K^+\mu^+\mu^-$ decay. *Eur. Phys. J. C* **2017**, *77*, 161. [CrossRef]
37. Adachi, I.; Adamczyk, K.; Aggarwal, L.; Ahmed, H.; Aihara, H.; Akopov, N.; Aloisio, A.; Ky, N.A.; Asner, D.; Atmacan, H.; et al. Evidence for $B^+ \to K^+\nu\bar{\nu}$ Decays. *arXiv* **2023**, arXiv:2311.14647. [CrossRef]
38. Parrott, W.G.; Bouchard, C.; Davies, C.T.H. Standard Model predictions for B→K$\ell^+\ell^-$, B→K$\ell_1^-\ell_2^+$ and B→K$\nu\bar{\nu}$ using form factors from $N_f = 2 + 1 + 1$ lattice QCD. *Phys. Rev. D* **2023**, *107*, 014511; Erratum in *Phys. Rev. D* **2023**, *107*, 119903. [CrossRef]
39. Chen, K.F.; Mombächer, T.; de Sanctis, U. Analysis of $B^0_{(s)} \to \mu^+\mu^-$ decays at the LHC. *arXiv* **2024**, arXiv:2402.09901. [CrossRef]
40. Frau, G.; Langenbruch, C. Charged Lepton-Flavour Violation. *Symmetry* **2024**, *16*, 359. [CrossRef]
41. Aaij, R.; Beteta, C.A.; Ackernley, T.; Adeva, B.; Adinolfi, M.; Afsharnia, H.; Aidala, C.A.; Aiola, S.; Ajaltouni, Z.; Akar, S.; et al. Measurement of CP-Averaged Observables in the $B^0 \to K^{*0}\mu^+\mu^-$ Decay. *Phys. Rev. Lett.* **2020**, *125*, 011802. [CrossRef]
42. Aaboud, M.; Angelozzi, I.; Bentvelsen, S.; Berge, D.; Bobbink, G.J.; Brenner, L.; Colijn, A.P.; de Groot, N.; de Jong, P.J.; Ferrari, P.; et al. Angular analysis of $B^0_d \to K^*\mu^+\mu^-$ decays in pp collisions at $\sqrt{s} = 8$ TeV with the ATLAS detector. *J. High Energy Phys.* **2018**, *2018*, 47. [CrossRef]
43. Sirunyan, A.M.; Tumasyan, A.; Adam, W.; Ambrogi, F.; Asilar, E.; Bergauer, T.; Brandstetter, J.; Brondolin, E.; Dragicevic, M.; Erö, J.; et al. Measurement of angular parameters from the decay $B^0 \to K^{*0}\mu^+\mu^-$ in proton-proton collisions at $\sqrt{s} = 8$ TeV. *Phys. Lett. B* **2018**, *781*, 517–541. [CrossRef]
44. Wehle, S.; Niebuhr, C.; Yashchenko, S.; Adachi, I.; Aihara, H.; Al Said, S.; Asner, D.; Aulchenko, V.; Aushev, T.; Ayad, R.; et al. Lepton-Flavor-Dependent Angular Analysis of $B \to K^*\ell^+\ell^-$. *Phys. Rev. Lett.* **2017**, *118*, 111801. [CrossRef] [PubMed]
45. Aaij, R.; Abellán Beteta, C.; Ackernley, T.; Adeva, B.; Adinolfi, M.; Afsharnia, H.; Aidala, C.A.; Aiola, S.; Ajaltouni, Z.; Akar, S.; et al. Strong constraints on the $b \to s\gamma$ photon polarisation from $B^0 \to K^{*0}e^+e^-$ decays. *J. High Energy Phys.* **2020**, *2020*, 81. [CrossRef]
46. Aaij, R.; Beteta, C.A.; Ackernley, T.; Adeva, B.; Adinolfi, M.; Afsharnia, H.; Aidala, C.A.; Aiola, S.; Ajaltouni, Z.; Akar, S.; et al. Angular Analysis of the $B^+ \to K^{*+}\mu^+\mu^-$ Decay. *Phys. Rev. Lett.* **2021**, *126*, 161802. [CrossRef] [PubMed]
47. Sirunyan, A.M.; Tumasyan, A.; Adam, W.; Bergauer, T.; Dragicevic, M.; Escalante Del Valle, A.; Fruehwirth, R.; Jeitler, M.; Krammer, N.; Lechner, L.; et al. Angular analysis of the decay $B^+ \to K^*(892)^+\mu^+\mu^-$ in proton-proton collisions at $\sqrt{s} = 8$ TeV. *J. High Energy Phys.* **2021**, *2021*, 124. [CrossRef]

48. Aaij, R.; Abdelmotteleb, A.S.W.; Abellán Beteta, C.; Ackernley, T.; Adeva, B.; Adinolfi, M.; Afsharnia, H.; Agapopoulou, C.; Aidala, C.A.; Aiola, S.; et al. Angular analysis of the rare decay $B_s^0 \to \phi\mu^+\mu^-$. *J. High Energy Phys.* **2021**, *2021*, 43. [CrossRef]
49. Aaij, R.; Adeva, B.; Adinolfi, M.; Affolder, A.; Ajaltouni, Z.; Albrecht, J.; Alessio, F.; Alexander, M.; Ali, S.; Alkhazov, G.; et al. Angular analysis of charged and neutral $B \to K\mu^+\mu^-$ decays. *J. High Energy Phys.* **2014**, *2014*, 82. [CrossRef]
50. Sirunyan, A.M.; Tumasyan, A.; Adam, W.; Ambrogi, F.; Asilar, E.; Bergauer, T.; Brandstetter, J.; Brondolin, E.; Dragicevic, M.; Erö, J.; et al. Angular analysis of the decay $B^+ \to K^+\mu^+\mu^-$ in proton-proton collisions at $\sqrt{s} = 8$ TeV. *Phys. Rev. D* **2018**, *98*, 112011. [CrossRef]
51. Descotes-Genon, S.; Hofer, L.; Matias, J.; Virto, J. On the impact of power corrections in the prediction of $B \to K^*\mu^+\mu^-$ observables. *J. High Energy Phys.* **2014**, *2014*, 125. [CrossRef]
52. Bobeth, C.; Chrzaszcz, M.; van Dyk, D.; Virto, J. Long-distance effects in $B \to K^*\ell\ell$ from analyticity. *Eur. Phys. J. C* **2018**, *78*, 451. [CrossRef]
53. Gubernari, N.; Reboud, M.; van Dyk, D.; Virto, J. Dispersive analysis of $B \to K^{(*)}$ and $B_s \to \phi$ form factors. *J. High Energy Phys.* **2023**, *2023*, 153. [CrossRef]
54. Aaij, R.; Abdelmotteleb, A.S.W.; Beteta, C.A.; Abudinén, F.; Ackernley, T.; Adeva, B.; Adinolfi, M.; Adlarson, P.; Agapopoulou, C.; Aidala, C.A.; et al. Amplitude analysis of the $B^0 \to K^{*0}\mu^+\mu^-$ decay. *Phys. Rev. D* **2023**, *102*, 112003. [CrossRef]
55. Hadavizadeh, T. $b \to s\ell\ell$ Decays at LHCb; Conference Talk on Behalf of the LHCb Collaboration Moriond QCD 2024. Available online: https://cds.cern.ch/record/2894566/files/Hadavizadeh.pdf (accessed on 9 May 2024).
56. Aaij, R.; Abdelmotteleb, A.; Abellan Beteta, C.; Abudinén, F.; Ackernley, T.; Adeva, B.; Adinolfi, M.; Adlarson, P.; Afsharnia, H.; Agapopoulou, C.; et al. Measurement of lepton universality parameters in $B^+ \to K^+\ell^+\ell^-$ and $B^0 \to K^{*0}\ell^+\ell^-$ decays. *Phys. Rev. D* **2023**, *108*, 032002. [CrossRef]
57. Aaij, R.; Beteta, C.A.; Ackernley, T.; Adeva, B.; Adinolfi, M.; Afsharnia, H.; Aidala, C.A.; Aiola, S.; Ajaltouni, Z.; Akar, S.; et al. Test of lepton universality in beauty-quark decays. *Nat. Phys.* **2022**, *18*, 277–282; Addendum: *Nat. Phys.* **2023**, *19*, 1517. [CrossRef]
58. Aaij, R.; Abellán Beteta, C.; Ackernley, T.; Adeva, B.; Adinolfi, M.; Afsharnia, H.; Aidala, C.; Aiola, S.; Ajaltouni, Z.; Akar, S.; et al. Test of lepton universality with $\Lambda_b^0 \to pK^-\ell^+\ell^-$ decays. *J. High Energy Phys.* **2020**, *2020*, 40. [CrossRef]
59. Aaij, R.; Abdelmotteleb, A.S.W.; Abellán Beteta, C.; Abudinén, F.; Ackernley, T.; Adeva, B.; Adinolfi, M.; Afsharnia, H.; Agapopoulou, C.; Aidala, C.A.; et al. Tests of lepton universality using $B^0 \to K_S^0\ell^+\ell^-$ and $B^+ \to K^{*+}\ell^+\ell^-$ decays. *Phys. Rev. Lett.* **2022**, *128*, 191802. [CrossRef]
60. Aaij, R.; Adeva, B.; Adinolfi, M.; Ajaltouni, Z.; Akar, S.; Albrecht, J.; Alessio, F.; Alexander, M.; Ali, S.; Alkhazov, G.; et al. Test of lepton universality with $B^0 \to K^{*0}\ell^+\ell^-$ decays. *J. High Energy Phys.* **2017**, *2017*, 55. [CrossRef]
61. Wehle, S.; Adachi, I.; Adamczyk, K.; Aihara, H.; Asner, D.; Atmacan, H.; Aulchenko, V.; Aushev, T.; Ayad, R.; Babu, V.; et al. Test of Lepton-Flavor Universality in $B \to K^*\ell^+\ell^-$ Decays at Belle. *Phys. Rev. Lett.* **2021**, *126*, 161801. [CrossRef]
62. Lees, J.; Poireau, V.; Tisserand, V.; Tico, J.G.; Grauges, E.; Palano, A.; Eigen, G.; Stugu, B.; Brown, D.N.; Kerth, L.; et al. Measurement of Branching Fractions and Rate Asymmetries in the Rare Decays $B \to K^{(*)}l^+l^-$. *Phys. Rev. D* **2012**, *86*, 032012. [CrossRef]
63. Choudhury, S.; Sandilya, S.; Trabelsi, K.; Giri, A.; Aihara, H.; Al Said, S.; Asner, D.; Atmacan, H.; Aulchenko, V.; Aushev, T.; et al. Test of lepton flavor universality and search for lepton flavor violation in $B \to K\ell\ell$ decays. *J. High Energy Phys.* **2021**, *2021*, 105. [CrossRef]
64. Hurth, T.; Mahmoudi, F.; Neshatpour, S. B anomalies in the post $R_{K^{(*)}}$ era. *Phys. Rev. D* **2023**, *108*, 115037. [CrossRef]
65. Greljo, A.; Salko, J.; Smolkovič, A.; Stangl, P. Rare b decays meet high-mass Drell-Yan. *J. High Energy Phys.* **2023**, *2023*, 87. [CrossRef]
66. Isidori, G.; Lancierini, D.; Owen, P.; Serra, N. On the significance of new physics $b \to s\ell^+\ell^-$ decays. *Phys. Lett. B* **2021**, *822*, 136644. [CrossRef]
67. Ciuchini, M.; Fedele, M.; Franco, E.; Paul, A.; Silvestrini, L.; Valli, M. Constraints on lepton universality violation from rare B decays. *Phys. Rev. D* **2023**, *107*, 055036. [CrossRef]
68. Capdevila, B.; Crivellin, A.; Descotes-Genon, S.; Hofer, L.; Matias, J. Searching for New Physics with $b \to s\tau^+\tau^-$ processes. *Phys. Rev. Lett.* **2018**, *120*, 181802. [CrossRef] [PubMed]
69. Lees, J.; Poireau, V.; Tisserand, V.; Tico, J.G.; Grauges, E.; Palano, A.; Eigen, G.; Stugu, B.; Brown, D.N.; Kerth, L.; et al. Evidence for an excess of $\bar{B} \to D^{(*)}\tau^-\bar{\nu}_\tau$ decays. *Phys. Rev. Lett.* **2012**, *109*, 101802. [CrossRef] [PubMed]
70. Lees, J.P.; Poireau, V.; Tisserand, V.; Grauges, E.; Palano, A.; Eigen, G.; Stugu, B.; Brown, D.N.; Kerth, L.T.; Kolomensky, Y.G.; et al. Measurement of an excess of $\bar{B} \to D^{(*)}\tau^-\bar{\nu}_\tau$ decays and implications for charged Higgs bosons. *Phys. Rev. D* **2013**, *88*, 072012. [CrossRef]
71. Sato, Y.; Iijima, T.; Adamczyk, K.; Aihara, H.; Asner, D.; Atmacan, H.; Aushev, T.; Ayad, R.; Aziz, T.; Babu, V.; et al. Measurement of the branching ratio of $\bar{B}^0 \to D^{*+}\tau^-\bar{\nu}_\tau$ relative to $\bar{B}^0 \to D^{*+}\ell^-\bar{\nu}_\ell$ decays with a semileptonic tagging method. *Phys. Rev. D* **2016**, *94*, 072007. [CrossRef]
72. Huschle, M.; Kuhr, T.; Heck, M.; Goldenzweig, P.; Abdesselam, A.; Adachi, I.; Adamczyk, K.; Aihara, H.; Al Said, S.; Arinstein, K.; et al. Measurement of the branching ratio of $\bar{B} \to D^{(*)}\tau^-\bar{\nu}_\tau$ relative to $\bar{B} \to D^{(*)}\ell^-\bar{\nu}_\ell$ decays with hadronic tagging at Belle. *Phys. Rev. D* **2015**, *92*, 072014. [CrossRef]
73. Caria, G.; Urquijo, P.; Adachi, I.; Aihara, H.; Said, S.A.; Asner, D.; Atmacan, H.; Aushev, T.; Babu, V.; Badhrees, I.; et al. Measurement of $\mathcal{R}(D)$ and $\mathcal{R}(D^*)$ with a semileptonic tagging method. *Phys. Rev. Lett.* **2020**, *124*, 161803. [CrossRef] [PubMed]

74. Hirose, S.; Iijima, T.; Adachi, I.; Adamczyk, K.; Aihara, H.; Al Said, S.; Asner, D.; Atmacan, H.; Aushev, T.; Ayad, R.; et al. Measurement of the τ lepton polarization and $R(D^*)$ in the decay $\bar{B} \to D^* \tau^- \bar{\nu}_\tau$ with one-prong hadronic τ decays at Belle. *Phys. Rev. D* **2018**, *97*, 012004. [CrossRef]
75. Aaij, R.; Abdelmotteleb, A.S.W.; Beteta, C.A.; Abudinén, F.; Ackernley, T.; Adeva, B.; Adinolfi, M.; Adlarson, P.; Afsharnia, H.; Agapopoulou, C.; et al. Test of lepton flavor universality using $B^0 \to D^{*-} \tau^+ \nu\tau$ decays with hadronic τ channels. *Phys. Rev. D* **2023**, *108*, 012018. [CrossRef]
76. Aaij, R.; Abdelmotteleb, A.S.; Beteta, C.A.; Abudinén, F.; Ackernley, T.; Adeva, B.; Adinolfi, M.; Adlarson, P.; Afsharnia, H.; Agapopoulou, C.; et al. Measurement of the ratios of branching fractions $\mathcal{R}(D^*)$ and $\mathcal{R}(D^0)$. *Phys. Rev. Lett.* **2023**, *131*, 111802. [CrossRef] [PubMed]
77. Amhis, Y.; Banerjee, S.; Ben-Haim, E.; Bertholet, E.; Bernlochner, F.U.; Bona, M.; Bozek, A.; Bozzi, C.; Brodzicka, J.; Chobanova, V.; et al. Averages of *b*-hadron, *c*-hadron, and τ-lepton properties as of 2021. *Phys. Rev. D* **2023**, *107*, 052008. [CrossRef]
78. Bordone, M.; Isidori, G.; Mächler, S.; Tinari, A. Short- vs. long-distance physics in $B \to K^{(*)} \ell^+ \ell^-$: A data-driven analysis. *arXiv* **2024**, arXiv:2401.18007.
79. Aaij, R.; Adeva, B.; Adinolfi, M.; Ajaltouni, Z.; Akar, S.; Albrecht, J.; Alessio, F.; Alexander, M.; Ali, S.; Alkhazov, G.; et al. Observation of the suppressed decay $\Lambda_b^0 \to p\pi^- \mu^+ \mu^-$. *J. High Energy Phys.* **2017**, *2017*, 29. [CrossRef]
80. Aaij, R.; Beteta, C.A.; Adametz, A.; Adeva, B.; Adinolfi, M.; Adrover, C.; Affolder, A.; Ajaltouni, Z.; Albrecht, J.; Alessio, F.; et al. First observation of the decay $B^+ \to \pi^+ \mu^+ \mu^-$. *J. High Energy Phys.* **2012**, *2012*, 125. [CrossRef]